Hydrogen solubility and diffusion in the shape-memory alloy NiTi

1989 J. Phys.: Condens. Matter 1 2473

(http://iopscience.iop.org/0953-8984/1/14/003)

J. Phys.: Condens. Matter 1 (1989) 2473–2482. Printed in the UK

Hydrogen solubility and diffusion in the shape-memory alloy NiTi

R Schmidt†, M Schlereth†, H Wipf†, W Assmus‡ and M Müllner§

† Institut für Festkörperphysik, Technische Hochschule Darmstadt, D-6100 Darmstadt, Federal Republic of Germany

‡ Physikalisches Institut, Universität Frankfurt, D-6000 Frankfurt, Federal Republic of Germany

§ Institut für Kernphysik, Universität Frankfurt, D-6000 Frankfurt, Federal Republic of Germany

Received 12 August 1988

Abstract. The solubility and the diffusion coefficient of hydrogen were determined in the austenitic (cubic) high-temperature phase of the shape-memory alloy NiTi. The measurements were made between 500 and 950 °C, with hydrogen gas pressures of up to 1.3 bar, and with hydrogen-to-NiTi ratios of up to 0.027. The hydrogen was in interstitial solid solution. The absorption process is exothermic. The enthalpy of solution per hydrogen atom is -183 ± 40 meV. The diffusion coefficient can be described by an Arrhenius relation with an activation energy $E = 480 \pm 50$ meV and a pre-exponential factor $D_0 = (4.7\ ^{+3.9}_{-2.5}) \times 10^{-3}\ \mathrm{cm^2\,s^{-1}}$.

NiTi hydride was synthesised in experiments with a higher hydrogen gas pressure (p = 150 bar, $T = 500$ K). Because of its brittleness, the hydride is readily pulverised by mechanical methods. This yields, after extraction of the hydrogen, NiTi powder which is difficult to prepare by other experimental techniques.

1. Introduction

NiTi is the technologically most important and experimentally most intensively studied shape-memory alloy. The memory behaviour is the result of a thermo-elastic martensitic phase transformation. The transition from the austenitic high-temperature phase (cubic CsCl structure) to the martensitic low-temperature phase (monoclinic) occurs, for equi-atomic stoichiometry, close above room temperature at about 40 °C. The transformation is accompanied by intermediate (pre-martensitic) phases, by strong hysteresis effects and by anomalies in the physical properties (e.g. electrical resistivity and softening of acoustic phonon branches). Details of both the metallurgy and the phase transformations of the alloy system NiTi have been discussed in [1–7] and references therein.

In the present paper, we report first on the results of experiments in which we determined the solubility and the diffusion coefficient of hydrogen interstitials in the austenitic high-temperature phase of equi-atomic NiTi. The experiments were performed in the temperature range between 500 and 950 °C, in the interstitial solid solution range at low hydrogen concentrations up to a hydrogen-to-NiTi ratio x of 0.027. Chief motivation for the study was that the temperature of the martensitic transformation in

0953-8984/89/142473 + 10 $02.50

NiTi varies sensitively with both stoichiometry and impurity content. Doping with hydrogen is, therefore, expected to represent a promising means of adjusting the transformation temperature reversibly. To achieve this in a reproducible and predictable way requires, however, knowledge of both the solubility and the diffusion coefficient of the hydrogen.

A second aspect addressed in this paper is that NiTi hydride, which is formed at high hydrogen concentrations, can readily be pulverised because of its mechanical brittleness (e.g. in a mortar). This yields, after extraction of the hydrogen, NiTi powder which is difficult to produce by other experimental techniques. In the present study, we prepared NiTi hydride by exposing solid NiTi to a hydrogen gas atmosphere at a high pressure (150 bar). Although powder preparation via hydriding is an established metallurgical technique, for instance in permanent magnet production [8], we present in this paper an x-ray diffraction spectrum of our NiTi powder in order to demonstrate the applicability of the hydride pulverisation method also to this system.

Reports on previous studies of the behaviour of hydrogen in NiTi have been given in [9–13]. The studies concentrated essentially on the solubility of the hydrogen in hydride phases, i.e. in the range of high hydrogen concentrations. They do not contain quantitative information on the interstitial solid solution range at low hydrogen concentrations, which is the preferred topic of investigation in the present study (α-phase). Neither do the studies in [9–13] provide information on the diffusion coefficient of hydrogen. It may, however, be anticipated that hydrogen in NiTi exhibits similarities to its behaviour in the isostructural hydrogen-storage alloy FeTi (at least in the interstitial solid solution range) [14–16]. By conclusion from analogy, it may be suspected that hydrogen in both NiTi and FeTi occupies the same type of octahedral interstitial site (half-way between two nickel or iron atoms [14]), and such a conclusion also suggests that a similar diffusion behaviour can be assumed. Our present results do, indeed, support this assumption.

2. Sample preparation and experimental details

Our measurements were performed on two NiTi cylinders (sample 1 of radius 3.9 mm and length 24.5 mm; sample 2 of radius 4.5 mm and length 19 mm). The cylinders were prepared from equi-atomic amounts of nickel (99.99% pure) and titanium (99.97% pure) rods by arc melting in an argon atmosphere. For homogenisation, they were subsequently kept for several hours above the melting point (1240 °C) in a levitation furnace under vacuum conditions (10^{-5} mbar). The precise cylindrical shape was achieved by spark erosion. The cylinders were finally electropolished in a solution of 3% perchloric acid in methanol.

The solubility of the hydrogen in solid solution was determined from pressure–composition isotherms taken in an UHV system. The investigated NiTi sample was in a temperature-controlled chamber (with a volume of about 220 cm^3, a temperature stability of 0.3 K, and absolute accuracy between ± 15 and ± 20 K) which was part of that system and could be connected to calibrated standard volumes of 224 cm^3 and 1008 cm^3, respectively. The hydrogen gas admitted to the system was purified in a palladium permeation cell (presures up to 1.3 bar). The pressure of the hydrogen atmosphere in the sample chamber and in the standard volumes was measured by sensitive differential membrane manometers (accuracy down to 0.05 mbar). The measurement of the hydrogen gas pressure allowed, with the help of the standard volumes, precise determination

of the total amount of hydrogen gas in the system and, therefore, also of the hydrogen concentration in the sample.

The diffusion coefficient of the hydrogen in NiTi was derived from the time dependence of the hydrogen pressure in the above vacuum system during an absorption process that was initiated by admission of a given amount of hydrogen gas. Such an experimental procedure requires that surface barrier effects are negligible in order to investigate truly bulk diffusion behaviour. For this reason, the majority of the measurements, particularly below 750 °C, were carried out after our samples had been coated by sputtering with a palladium layer 1–2 μm thick. This will be discussed in more detail in § 4.

The preparation of NiTi hydride in order to demonstrate the pulverisation method was carried out at 500 °C in a (separate) vacuum system that was designed for hydrogen gas pressures up to 200 bar. The hydriding pressure was 150 bar, and the total hydrogen concentrations x determined by heat extraction ranged from 1.26 to 1.34. The NiTi hydride was pulverised in a mortar. The NiTi powder grains used for the x-ray diffraction measurements were limited in their diameter with the help of sieves to the range between 20 and 70 μm. The hydrogen extraction after pulverisation was performed at 900 °C in a vacuum of 10^{-6} mbar.

3. Hydrogen solubility

Figure 1 presents four of our pressure–composition isotherms obtained in the temperature range between 500 and 950 °C. Within experimental accuracy, the concentration x is found to vary, for each isotherm, linearly with the square root of the hydrogen gas pressure p. This represents an ideal solution behaviour which agrees with Sieverts' law and demonstrates that hydrogen–hydrogen interaction effects are negligible in the investigated range of low hydrogen concentrations ($x \leqslant 0.027$) [17, 18]. For a given hydrogen pressure p, the equilibrium concentration increases further with falling temperature. This shows that the solution of hydrogen gas in NiTi is an exothermic process.

The absorption behaviour of the hydrogen is quantitatively described by the partial enthalpy of solution Δh_H and the partial (non-configurational) entropy $\Delta s_H^{(nc)}$ of solution. Thermodynamic equilibrium requires, for a given temperature T, identical chemical potentials of the hydrogen in the gaseous state and in solid solution. In the gaseous state, the chemical potential per hydrogen atom can be written as

$$\mu_{H_2}(p, T) = \tfrac{1}{2}[h_{H_2}^{(0)} - Ts_{H_2}^{(0)}] + \tfrac{1}{2}k_B T \ln(p/p_0) \tag{1}$$

whereas, in solid solution, it is given by [17, 18]

$$\mu_H(x, T) = h_H - Ts_H^{(nc)} + k_B T \ln(x/x_0). \tag{2}$$

The first of the two equations presupposes ideal behaviour of the hydrogen gas which seems appropriate in view of the temperatures and the moderate pressures of this investigation ($p \leqslant 1.3$ bar). $h_{H_2}^{(0)}$ is the enthalpy and $s_{H_2}^{(0)}$ is the entropy of a hydrogen molecule for a standard reference pressure $p = p_0 = 1$ atm = 1.013 25 bar. k_B is Boltzmann's constant. In the second equation, h_H is the partial enthalpy of a hydrogen atom in solid solution, and $s_H^{(nc)}$ is the non-configurational part of its partial entropy. The final term in this equation accounts for the configurational part $s_H^{(c)} = -k_B \ln(x/x_0)$ of the partial entropy, where x_0 represents—per NiTi formula unit—the number of interstitial sites that can be occupied by the hydrogen atoms. The configurational part of the partial

entropy, as given above (and in equation (2)), applies to small hydrogen concentrations ($x \ll x_0$). This corresponds to the situation in our experiments. In the general case, the configurational part of the partial entropy is conventionally written as $s_H^{(c)} = -k_B \ln[x/(x_0 - x)]$ since a given interstitial site is considered to be occupied by not more than one hydrogen atom.

A definite separation of the partial entropy in its configurational and non-configurational parts requires knowledge of the value of x_0, i.e. of the types of interstitial site occupied by the hydrogen. If we presuppose that hydrogen in NiTi occupies the same (octahedral) sites as in FeTi [14], x_0 assumes a value of 3 which will be used in our subsequent discussion. We note finally that the non-configurational partial entropy can, in principle, be calculated absolutely from physical properties of the considered metal–hydrogen system (hydrogen-induced modifications of the electronic specific heat and the lattice vibrations) [19, 20]. Knowledge of these properties, which are not available for the present system $NiTiH_x$, therefore allows determination of x_0 from experimental hydrogen solubility data. The condition of identical chemical potentials of the hydrogen in the gaseous state and in solid solution yields, according to equations (1) and (2), the relation

$$x/x_0 = \sqrt{p/p_0} \exp(-\Delta h_H/k_B T) \exp(\Delta s_H^{(nc)}/k_B) \tag{3}$$

between the concentration x and the hydrogen gas pressure p. In this equation, $\Delta h_H = h_H - \frac{1}{2}h_{H_2}^{(0)}$ is the partial enthalpy of solution, and $\Delta s_H^{(nc)} = s_H^{(nc)} - \frac{1}{2}s_{H_2}^{(0)}$ is the partial non-configurational entropy of solution. A negative value of Δh_H describes an exothermic solution behaviour. As discussed before, the value of $\Delta s_H^{(nc)}$ is correlated to the value of 3 that we selected for x_0. If x_0 actually differs from 3, $\Delta s_H^{(nc)}$ has to be augmented by $k_B \ln(3/x_0)$.

The quantities Δh_H and $\Delta s_H^{(nc)}$ in equation (3) vary, in general, with concentration x and temperature T. For a given x and T, Δh_H can be determined from the van't Hoff equation [17]

$$\Delta h_H = (k_B/2)[\partial(\ln p)/\partial(1/T)]_x \tag{4}$$

where the subscript x denotes differentiation with a constant concentration x. The isotherms in figure 1, which exhibit a linear relationship between $\sqrt{p}$ and x (Sieverts' law [17, 18]), demonstrate accordingly that Δh_H is independent of x, at least for a given temperature and within experimental accuracy. Figure 2 shows p/p_0 logarithmically plotted against $1/T$ where p represents the equilibrium hydrogen gas pressure required for a concentration $x = 0.01$ that is well within the investigated concentration range ($0 < x \leq 0.027$). The respective equilibrium values for p were taken from the slope of all our absorption isotherms, such as indicated in figure 1 in the case of the four isotherms presented there. For a given temperature, the enthalpy Δh_H of solution is, according to equation (4), determined from the slope of the data presented in figure 2. The data in this figure yield the result $\Delta h_H = -183 \pm 40$ meV. This result is, within experimental accuracy, independent of both temperature and concentration.

The negative value of Δh_H demonstrates the exothermic solution behaviour of hydrogen gas in the solid solution (low-concentration) range of $NiTiH_x$. This behaviour differs from the endothermic behaviour found in the solid solution range of the isostructural hydrogen storage alloy $FeTiH_x$ ($\Delta h_H \simeq 110$ meV [16]).

Once Δh_H is derived, equation (3) allows the determination of the non-configurational partial entropy of solution $\Delta s_H^{(nc)}$ from the data in figure 2. Our result for this quantity is $\Delta s_H^{(nc)} = -0.63 \pm 0.04$ meV K^{-1}. Within experimental accuracy, $\Delta s_H^{(nc)}$ is

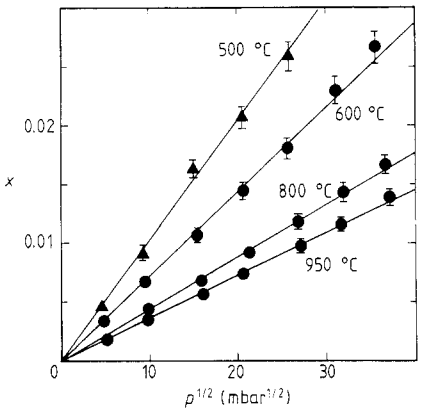

Figure 1. Pressure–composition isotherms for hydrogen in NiTi. For four temperatures, the hydrogen-to-NiTi ratio x is plotted against the square root of the hydrogen gas pressure p: ▲, data for sample 1; ●, data for sample 2.

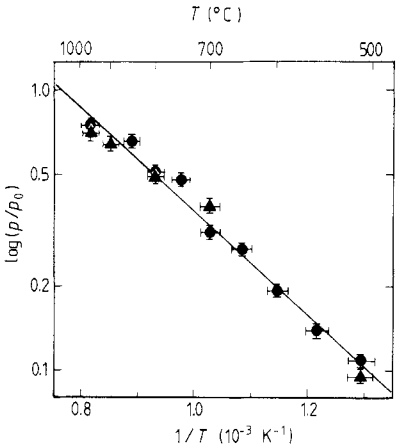

Figure 2. Logarithmic plot of p/p_0 against reciprocal temperature T: ▲, data for sample 1; ●, data for sample 2. p is the equilibrium hydrogen gas pressure required for a concentration $x = 0.01$, and $p_0 = 1.013\,25$ bar is the standard reference pressure.

found to be independent of concentration x and temperature T. This follows from the validity of Sieverts' law and from the fact that Δh_H does not noticeably vary with x and T. We note, for comparison, that the value of $\Delta s_H^{(nc)}$ for the system $NiTiH_x$ is somewhat more negative than that reported for $FeTiH_x$ ($\Delta s_H^{(nc)} \simeq -0.4$ meV K^{-1} in the solid solution range [16]).

Our present results $\Delta h_H = -183 \pm 40$ meV and $\Delta s_H^{(nc)} = -0.63 \pm 0.04$ meV K^{-1} allow, according to equation (3), the quantitative calculation of the p–x–T relationship in the investigated pressure, composition and temperature range. We give also the subsequent numerical expression

$$x = 1.95 \times 10^{-3}\sqrt{p}\exp(2124/T) \tag{5}$$

which allows a direct calculation of x from the pressure p (bar) and the temperature T(K).

A final aspect which requires discussion is the possibility that, in the course of our experiments, the host alloy NiTi disintegrated owing to the presence of the hydrogen atmosphere [12, 21]. Such disintegration is well known to occur at high hydrogen concentrations (or pressures) in the storage alloy FeTi, where the formation of $FeTiH_2$ is thermodynamically less favourable than segregation into TiH_2 and $TiFe_2$. For hydrogen pressures above 40 bar, segregation into TiH_2 and $TiNi_3$ is also reported for the alloy system NiTi [12]. With respect to the present study, we can, however, safely exclude such segregation. Our absorption isotherms were taken at very low hydrogen concentrations ($x \leqslant 0.027$, i.e. less than 1.35 at.%) where, for entropy reasons, disintegration effects are thermodynamically unfavourable. The maximum hydrogen gas pressure was 1.3 bar which is well below the value of 40 bar above which segregation is reported to occur [12]. We found further, during our measurements, no change or degradation in the absorption behaviour with time as expected in the presence of segregation effects. In fact, we observed complete reversibility with respect to variation in both pressure and tem-

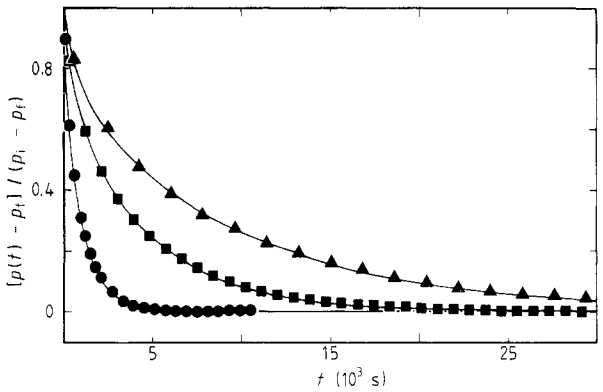

Figure 3. Hydrogen gas pressure $p(t)$ as a function of time t during absorption processes at three different temperatures: ▲, 500 °C; ■, 600 °C; ●, 800 °C. The pressure variation is shown in a normalised presentation where p_i and p_f are the pressure at the beginning ($t = 0$) and end ($t = \infty$) of the absorption process. The data were taken from sample 2. The full curves are fitted curves explained in the text.

perature. Finally, the diffusion measurements reported in § 4 demonstrated a time dependence of the absorption processes such as expected for pure bulk diffusion. This excludes the possibility of an absorption process whose kinetics are controlled by segregation. In view of all the reasons listed above, we conclude that disintegration effects did not take place in the course of the present study.

4. Diffusion coefficient of the hydrogen

Figure 3 presents, for three different temperatures, examples for the absorption-induced decrease in the hydrogen gas pressure in our vacuum system after hydrogen gas was admitted to the system at time $t = 0$. Before this admission, the system and the NiTi sample in it were free of hydrogen. The data in figure 3 show a distinct increase in the absorption rate with rising temperature as expected in the case of a diffusion-controlled absorption process, and for a diffusion coefficient which increases with temperature.

The time-dependent decrease in the pressure in figure 3 describes the amount of hydrogen gas absorbed by the sample. For an absorption process controlled by bulk diffusion, the average (time-dependent) hydrogen concentration $c(t)$ in an (infinitely) long cylindrical sample with radius r can be written as [22]

$$\frac{c(t)}{c_0} = 1 - \sum_{n=1}^{\infty} \left(\frac{2}{\sigma_n}\right)^2 \exp\left(-\sigma_n \frac{Dt}{r^2}\right) \tag{6}$$

where c_0 is the concentration at the surface of the sample and D is the diffusion coefficient. The coefficients σ_n are the argument values at the zeros of the Bessel function $J_0(z)$ (e.g. $\sigma_1 = 2.405$, $\sigma_2 = 5.520$). Equation (6) describes the appropriate situation for the present experiments in which the sample originally ($t = 0$) was free of hydrogen, and where $c(t)$ is proportional to the amount of absorbed hydrogen.

If we presuppose diffusion-controlled hydrogen absorption, the pressure variations in figure 3 are described by the above equation. The full curves in this figure represent the fitted curves obtained under this assumption. The relevant fit parameter was the diffusion coefficient. The fitted curves provide an excellent description of the data which supports our presupposition of a diffusion-controlled absorption. This fact will again be addressed in this paper.

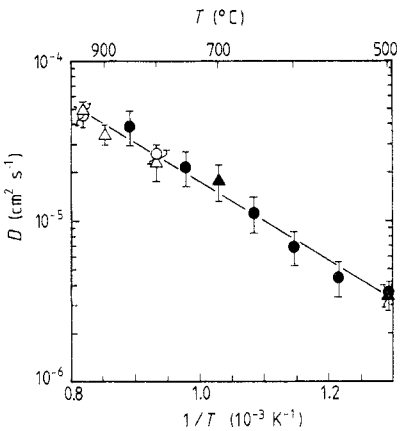

Figure 4. Arrhenius plot of the diffusion coefficient D of hydrogen in NiTi: ▲, △, data for sample 1; ●, ○, data for sample 2; ▲, ●, measurements in which the sample surface was coated with a thin (1–2 μm) palladium layer; △, ○, for uncoated NiTi samples.

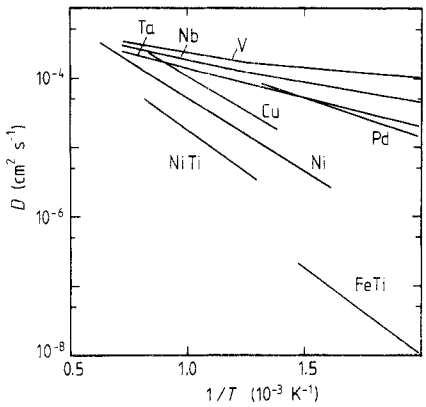

Figure 5. Arrhenius plot of the diffusion coefficient D of hydrogen in metals with BCC (vanadium, niobium and tantalum), FCC (palladium, copper and nickel), and CsCl structure (NiTi and FeTi). The NiTi data are present results, the FeTi data are from [15], and the other data are from [24, 25]. All data apply to low hydrogen concentrations.

An additional point which requires consideration is that our actual sample geometry differed from that of an infinitely long cylinder such as presupposed in equation (6). In fact, the end faces of our samples increase the absorption rate compared with this equation which simulates a larger diffusion coefficient. We performed, for both sample geometries, numerical calculations on the actual diffusion process which demonstrated that equation (6) is a nearly perfect description of the absorption rate provided that the value of the diffusion coefficient is increased by 7.4% (sample 1) or 12.0% (sample 2) [23]. Therefore, in order to determine the diffusion coefficient from our experiments, we made fits to our data with the help of equation (6) and corrected the value of the diffusion coefficient thus obtained for its apparent increase above.

Figure 4 presents our results for the diffusion coefficient of hydrogen in NiTi in a semi-logarithmic plot against reciprocal temperature. The results are valid for low hydrogen concentrations ($x \leqslant 0.027$). Each of the data points represents an average over three to seven absorption measurements performed with different hydrogen gas pressures (up to 1.3 bar). It is seen that the diffusion coefficient D is well described by the Arrhenius relation

$$D = D_0 \exp(-E/k_B T) \tag{7}$$

where E is the activation energy and D_0 is the pre-exponential factor. From a fit to the data in figure 4 (full curve), we find $E = 480 \pm 50$ meV and $D_0 = (4.7\ ^{+3.9}_{-2.5}) \times 10^{-3}$ cm^2 s^{-1}.

As pointed out in § 2, a prerequisite of the present experiments is that surface barrier effects can be neglected. In order to reduce the possible influence of such effects, our measurements were carried out under UHV conditions. Furthermore, they were made

in a range of relatively high temperatures ($T \geq 500$ °C) where surface effects are of less importance. In spite of these facts, we found in very early measurements intentionally performed at the most critical temperature of 500 °C that the absorption rate sometimes deviated from pure bulk diffusion behaviour as described by equation (6). In these cases, the absorption rate was also reduced, which clearly indicated the existence of a surface barrier. Although similar effects were not observed at higher temperatures, we decided to perform the actual measurements below 800 °C solely after the samples were coated by sputtering with a thin palladium layer (1–2 μm) in order to rule out completely the potential influence of surface barriers. The experiments at the highest temperatures were made, however, prior to this sputtering procedure in order to reduce inter-diffusion effects between the palladium coating and sample, and in order to prevent substantial palladium evaporation.

Our measurements on the palladium-coated samples indicated no deviations from bulk-diffusion-controlled absorption as presupposed in equation (6). For a given temperature, we found no variations in the absorption rate beyond the experimental accuracy. In the temperature range around 800 °C, where data were taken on both coated and uncoated samples, the results for their diffusion coefficients are identical within their experimental error. Figure 4 shows further that our data can be well described by an Arrhenius law from which, at lower temperatures, we would expect a (downward) deviation in the presence of surface barrier effects. For all these reasons, we judge that the results in figure 4 were indeed derived from absorption data controlled by bulk diffusion.

Finally, for comparison with other metallic systems, we present in figure 5 a compilation which shows the diffusion coefficient of hydrogen in metallic systems with BCC (vanadium, niobium and tantalum), FCC (palladium, copper and nickel) and CsCl structure (NiTi and FeTi). The figure reveals characteristic structural differences. The diffusion rate is, at low temperatures, quickest in BCC metals, and it becomes continuously smaller in FCC and CsCl structures. It is likely that this systematic behaviour can be attributed to that fact that the distance between nearest-neighbour interstitial sites occupied by the hydrogen in the individual structures increases in the same order [24, 25]. The fact that the two metallic systems with a CsCl structure, NiTi and FeTi, exhibit very similar diffusion rates with nearly identical activation energies seems particularly worth mentioning since it supports strongly our conclusion from analogy that hydrogen in NiTi occupies the same octahedral interstitial sites as in FeTi.

5. X-ray diffraction spectrum of NiTi powder

In order to demonstrate the potential of powder production by hydriding, we present in figure 6 an x-ray diffraction spectrum of NiTi powder taken at 80 °C with the Kα radiation of a copper anode ($\lambda_{K\alpha_1} = 1.5443$ Å; $\lambda_{K\alpha_2} = 1.5405$ Å). The spectrum shows the cubic CsCl structure of the austenitic high-temperature phase of NiTi. The lattice parameter derived from the spectrum is 3.015 Å in agreement with previous studies [3]. The small peak near the [110] peak is likely to result from untransformed martensite. Although we did not find direct evidence, we cannot exclude the possibility that disintegration effects took place in our $NiTiH_x$ sample in the course of the hydriding procedure (see discussion in § 3). These effects, if they occurred at all, were reversed, however, during the subsequent extraction of the hydrogen at 900 °C under vacuum conditions.

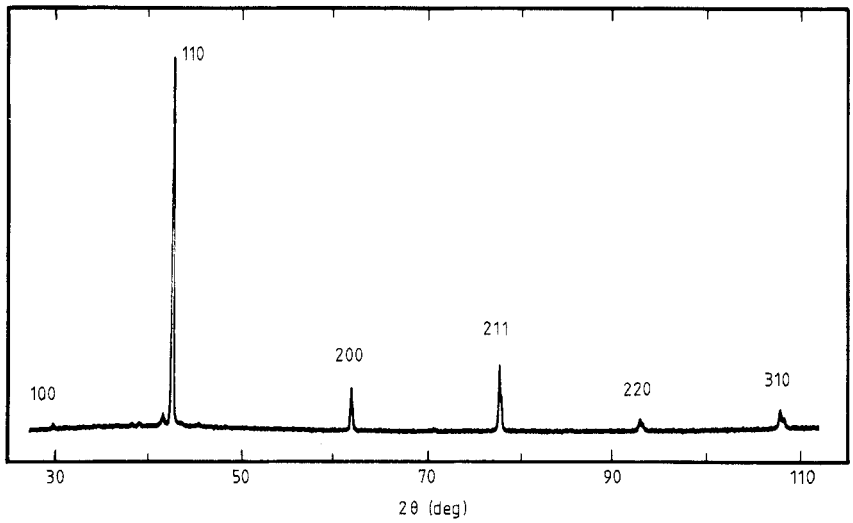

Figure 6. X-ray diffraction spectrum of NiTi powder taken at 80 °C (Cu Kα radiation; $\lambda_{K\alpha_1} = 1.5443$ Å; $\lambda_{K\alpha_2} = 1.5405$ Å).

6. Conclusions

Hydrogen dissolves exothermically in the austenitic high-temperature phase of NiTi. In the investigated ranges of temperature (770 K $< T <$ 1220 K), pressure ($p < 1.3$ bar) and concentration (hydrogen-to-NiTi ratio $x < 0.027$), the hydrogen is in interstitial solid solution and the p–x–T relationship is quantitatively given by $x = 1.95 \times 10^{-3}\sqrt{p}\exp(2124/T)$. In the same range of p, x and T, the diffusion coefficient $D = D_0\exp(-E/k_BT)$ of the hydrogen has an activation energy $E = 480 \pm 50$ meV and a pre-exponential factor $D_0 = (4.7\ ^{+3.9}_{-2.5}) \times 10^{-3}$ cm^2 s^{-1}.

NiTi hydride can be synthesised at high hydrogen pressures. It is brittle and can readily be pulverised. This fact provides a convenient method for the preparation of NiTi powder.

Acknowledgments

We would like to thank B Herth (Firma STOE) for his assistance in the x-ray diffraction measurements. The work was supported by the Bundesministerium für Forschung und Technologie under Contract 211-5291-03 WI 1 DAR-9.

References

[1] Philip T V and Beck P A 1957 *Trans. AIME* **209** 1269–71
[2] Delaey L and Chandrasekaran M (ed.) 1982 *J. Physique Coll.* **43** C4
[3] Bührer W, Gotthardt R, Kulik A, Mercier O and Staub F 1983 *J. Phys. F: Met. Phys.* **13** L77–81
[4] Tietze H, Müllner M and Renker B 1984 *J. Phys. C: Solid State Phys.* **17** L529–32

[5] Salamon M B, Meichle M E and Wayman C M 1985 *Phys. Rev.* B **31** 7306–15
[6] Tietze H, Müllner M, Selgert P and Assmus W 1985 *J. Phys. F: Met. Phys.* **15** 263–71
[7] Tamura I (ed.) 1986 *Proc. Int. Conf. Martensitic Transformations (Nara) 1986* (Tokyo: Japan Institute of Metals)
[8] Harris I R 1987 *J. Less-Common Met.* **131** 245–62
[9] Buchner H, Gutjahr M A, Beccu K-D and Säufferer H 1972 *Z. Metallk.* **63** 497–500
[10] Jackson C M, Wagner H J and Wasilewski R J 1972 *NASA Special Publication No* SP 5110 (Battelle Memorial Institute)
[11] Yamanaka K, Saito H and Someno M 1975 *Nippon Kagaku Kaishi* **8** 1267–72
[12] Buchner H 1982 *Energiespeicherung in Metallhydriden* (Berlin: Springer)
[13] Wulz H G and Fromm E 1986 *J. Less-Common Met.* **118** 315–26
[14] Thompson P, Reidinger F, Reilly J J, Corliss L M and Hastings J M 1980 *J. Phys. F: Met. Phys.* **10** L57–9
[15] Arnold N and Welter J-M 1983 *Metall. Trans.* A **14** 1573–7
[16] Welter J-M, Arnold G and Wenzl H 1983 *J. Phys. F: Met. Phys.* **13** 1773–84
[17] Mueller W M, Blackledge J P and Libowitz G G (ed.) 1968 *Metal Hydrides* (New York: Academic)
[18] Wicke E and Brodowsky H 1978 *Springer Topics in Applied Physics* vol 29, ed. G Alefeld and J Völkl (Berlin: Springer) pp 73–155
[19] Boureau G and Kleppa O J 1976 *J. Chem. Phys.* **65** 3915–20
[20] Magerl A, Stump N, Wipf H and Alefeld G 1977 *J. Phys. Chem. Solids* **38** 683–6
[21] Wiswall R 1978 *Springer Topics in Applied Physics* vol 29, ed. G Alefeld and J Völkl (Springer: Berlin) pp 201–42
[22] Jost W 1952 *Diffusion in Solids, Liquids and Gases* (New York: Academic)
[23] Schmidt R 1986 *Diploma Thesis* Technische Hochschule Darmstadt
[24] Völkl J and Alefeld G 1978 *Springer Topics in Applied Physics* vol 28, ed. G Alefeld and J Völkl (Berlin: Springer) pp 321–48
[25] Fukai Y and Sugimoto H 1985 *Adv. Phys.* **34** 263–326